

Proposal for optical parity state re-encoder

Y. X. Gong^{1,2,*}, A. J. F. Hayes¹, G. C. Guo² and T. C. Ralph¹

¹ Centre for Quantum Computer Technology, Department of Physics,
University of Queensland, St Lucia 4072, Australia

² Key Laboratory of Quantum Information, University of Science and Technology of China, CAS,
Hefei, 230026, People's Republic of China

(Dated: October 17, 2021)

We propose a re-encoder to generate a refreshed parity encoded state from an existing parity encoded state. This is the simplest case of the scheme by Gilchrist *et al.* (Phys. Rev. A 75, 052328). We show that it is possible to demonstrate with existing technology parity encoded quantum gates and teleportation.

PACS numbers: 03.67.Lx, 42.50.Dv, 42.79.Ta

I. INTRODUCTION

Linear optical quantum computing with single photon modes (LOQC) was novel and surprising, but not very practical when first introduced some years ago [1]. The idea was to restrict all in-line processing to linear optical networks and to use measurement induced non-linearities, additional single photon ancilla states and feedforward to produce the necessary two-qubit interactions. Although scalable in principle, the original scheme required an unacceptably high number of operations ($\approx 10,000$) to produce a near deterministic two-qubit gate. More recently much progress has been made in understanding and simplifying LOQC [2]. In particular two approaches, cluster states [3] and parity states [4], can achieve near deterministic two-qubit gates using approximately 100 operations.

Although near deterministic operation is still some way off, considerable success has been shown in demonstrating non-deterministic optical quantum gates and small scale circuits [5, 6, 7]. Progress has been made in demonstrating the principles of cluster state computation [8, 9], but only basic parity state demonstrations have so far been attempted [10, 11].

Here we propose an experimental scheme that could demonstrate the key features of parity state gate operation including loss error detection [12], and that should be practical with current down-conversion technology. The paper is arranged in the following way. In the next section we introduce the parity encoding and then describe the basic re-encoder demonstration in Section III. In Section IV we consider gate operations and then follow in Section V with a description of teleportation with the circuit. In Section VI we talk about the possible experimental implementation using parametric down-conversion processes, linear optical elements, and conventional photon detectors. Section VII analyzes the effect that optical mode-mismatch will have on the operation

of the gates and we conclude in Section VIII.

II. PARITY ENCODING

Parity encoding has been shown as an efficient way to protect against a computational basis measurement of one or more of the component qubits [1]. We will use the notation $|\Psi\rangle^{(n)}$ to represent the logical state $|\Psi\rangle$ which is parity encoded across n distinct qubits. Explicitly, for an arbitrary state $|\Psi\rangle = \alpha|0\rangle + \beta|1\rangle$, it can be parity encoded as $|\Psi\rangle^{(n)} = \alpha|0\rangle^{(n)} + \beta|1\rangle^{(n)}$. The even and odd parity states are given by

$$\begin{aligned} |0\rangle^{(n)} &\equiv \frac{1}{\sqrt{2}} \left(|+\rangle^{\otimes n} + |-\rangle^{\otimes n} \right) \\ |1\rangle^{(n)} &\equiv \frac{1}{\sqrt{2}} \left(|+\rangle^{\otimes n} - |-\rangle^{\otimes n} \right), \end{aligned} \quad (1)$$

where $|\pm\rangle = (|0\rangle \pm |1\rangle)/\sqrt{2}$. We can see that $|0\rangle^{(n)}$ is represented as an equal superposition of all states with even parity (the number of the component qubits in the $|1\rangle$ state is even), and that $|1\rangle^{(n)}$ is represented as an equal superposition of all states with odd parity (the number of the component qubits in the $|1\rangle$ state is odd). If a computational basis measurement is made on any of the component qubits, it will not destroy the logical state, but collapse the original state to $|\Psi\rangle^{(n-1)} = \alpha|0\rangle^{(n-1)} + \beta|1\rangle^{(n-1)}$ if the measurement result is “0”, otherwise if the measurement result is “1” the original state will collapse to $|\Phi\rangle^{(n-1)} = \alpha|1\rangle^{(n-1)} + \beta|0\rangle^{(n-1)}$, which can be corrected by a bit-flip on any of the remaining component qubits.

In this paper, we consider the simplest parity encoded state—two-qubit parity encoded state,

$$\begin{aligned} |\Psi\rangle^{(2)} &= \alpha|0\rangle^{(2)} + \beta|1\rangle^{(2)} \\ &= \frac{1}{\sqrt{2}} [\alpha(|00\rangle + |11\rangle) + \beta(|01\rangle + |10\rangle)]. \end{aligned} \quad (2)$$

We use the polarization states of a photon to construct the component qubits, so that $|0\rangle \equiv |H\rangle$ and $|1\rangle \equiv |V\rangle$.

*Electronic address: yxgong@mail.ustc.edu.cn

A straightforward way [13] to prepare the parity encoded state of an arbitrary state $|\Psi\rangle = \alpha|H\rangle + \beta|V\rangle$ is utilizing a controlled-not(CNOT) gate, with the photon in the state $|\Psi\rangle$ as the target and an ancilla photon in the state $(|H\rangle + |V\rangle)/\sqrt{2}$ as the control, which has been experimentally demonstrated [10]. A simpler way to generate a postselected parity encoded state is given by Pittman *et al.* [11], only using a single polarizing beam splitter(PBS) and an ancilla photon. Here we give another way to prepare the parity encoded state from the non-maximally entangled state. To show this we rewrite Eq. (2) as

$$\begin{aligned} |\Psi\rangle^{(2)} &= \frac{1}{\sqrt{2}}[\alpha(|++\rangle + |--\rangle) + \beta(|+-\rangle - |-+\rangle)] \\ &= \frac{1}{\sqrt{2}}[(\alpha + \beta)(|++\rangle) + (\alpha - \beta)|--\rangle] \\ &= A|++\rangle + B|--\rangle, \end{aligned} \quad (3)$$

where $A \equiv (\alpha + \beta)/\sqrt{2}$, $B \equiv (\alpha - \beta)/\sqrt{2}$, and $|\pm\rangle$ is the $\pm 45^\circ$ polarized state. Therefore we can first prepare a non-maximally entangled state $A|HH\rangle + B|VV\rangle$, implement a Hadamard gate on each of the photons and then the parity encoded state as shown in Eq. (3) is yielded.

III. THE RE-ENCODER

An important technique in the application of parity encoding is the re-encoder, i.e., to rebuild another parity encoded state from an existing parity encoded state. Gilchrist *et al.* [4] have given an efficient way using the type-I(f_I) fusion gate and the type-II(f_{II}) fusion gate,

$$H f_I(H \otimes H)|0\rangle^{(n)}|0\rangle^{(m)} \rightarrow \begin{cases} |0\rangle^{(m+n-1)} & \text{(success)} \\ - & \text{(failure)} \end{cases} \quad (4)$$

$$f_{II}|0\rangle^{(n)}|0\rangle^{(m)} \rightarrow \begin{cases} |0\rangle^{(m+n-2)} & \text{(success)} \\ |0\rangle^{(m-1)}|0\rangle^{(n-1)} & \text{(failure)} \end{cases}, \quad (5)$$

and each fusion succeeds with a probability of 1/2. In this paper we give a detailed analysis of the simplest case and investigate the property of the re-encoder.

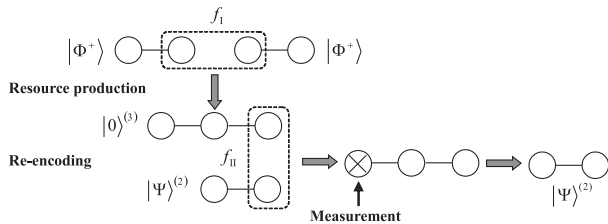


FIG. 1: Schematic of the re-encoder.

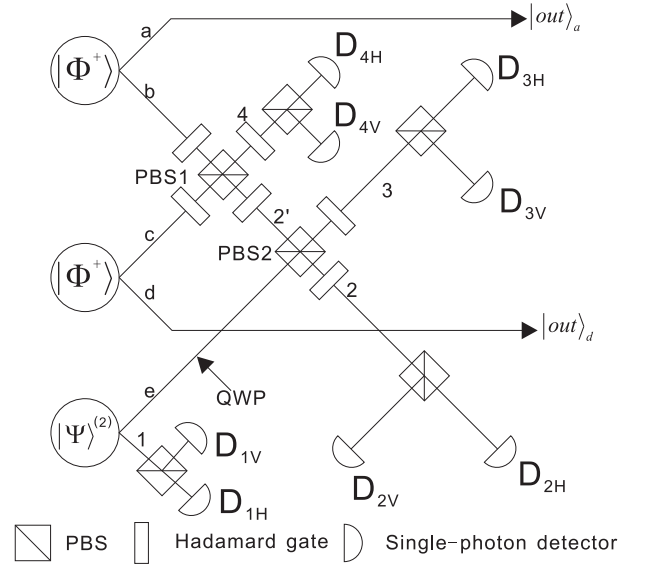


FIG. 2: Scheme to implement the two-photon parity state re-encoder. Lowercase letters and numbers label the beams. Polarizing beam splitters transmit horizontally polarized photons($|H\rangle$) and reflect vertically polarized photons($|V\rangle$). Hadamard gates transform horizontally polarized photons to $+45^\circ$ -polarized photons $|+\rangle$ and transform vertically polarized photons to -45° -polarized photons $|-\rangle$, which can be implemented by a half-wave plate oriented at 22.5° . A quarter-wave plate(QWP) set to 0° is inserted in beam e for implementing a Z_{90} gate on the photon in mode e .

Fig.1 shows the schematic of the re-encoder. We start from three entangled-photon pairs, two of which are in the Bell state $|\Phi^+\rangle = (|HH\rangle + |VV\rangle)/\sqrt{2}$, with the third one in the parity encoded state as shown in Eq. (3). We first assume that we have ideal entangled-photon sources and in Section VI we will talk about the generation of the entangled-photon pairs in real experiment. First we generate the resource state $|0\rangle^{(3)}$ from two Bell states using the f_I fusion gate. Second we fuse the original parity encoded state and the resource state using the f_{II} fusion gate. Third after projection measurement on the remaining photon of the original parity encoded state we produce a new parity encoded state.

Fig.2 shows the experimental scheme to demonstrate the re-encoder. To show the operation of the re-encoder we first consider the fusion between the two Bell states $|\Phi^+\rangle_{ab}$ and $|\Phi^+\rangle_{cd}$ at PBS1. The state transformation before PBS2 can be written as

$$\begin{aligned} |\Phi^+\rangle_{ab}|\Phi^+\rangle_{cd} \rightarrow & \frac{1}{4} [|H\rangle_a |H\rangle_d |H\rangle_{2'} + |H\rangle_a |V\rangle_d |V\rangle_{2'} \\ & + |V\rangle_a |V\rangle_d |H\rangle_{2'} + |V\rangle_a |H\rangle_d |V\rangle_{2'} \\ & + |V\rangle_a |H\rangle_d |H\rangle_{2'} + |H\rangle_a |V\rangle_d |H\rangle_{2'} \\ & + |H\rangle_a |H\rangle_d |V\rangle_{2'} + |V\rangle_a |V\rangle_d |V\rangle_{2'}] \\ & + \frac{1}{\sqrt{2}} |\varphi_1\rangle, \end{aligned} \quad (6)$$

where $|\varphi_I\rangle$ is a normalized combination of all the amplitudes that would not lead to exactly one photon in detectors D_{4H} and D_{4V} . If the detector D_{4H} receives exactly one photon the state in mode a , d , and $2'$ will collapse to $|0\rangle^{(3)}$, while if there is exactly one photon in D_{4V} the state will be $|1\rangle^{(3)}$, with a probability of $1/4$ for each result.

After the state $|0\rangle^{(3)}(|1\rangle^{(3)})$ is yielded, the photons in beams $2'$ and e are sent to PBS2, followed by detectors in beams 2 and 3, which act as a type-II fusion gate together with the PBS2. The whole state transformation can be written as

$$\begin{aligned}
|\Phi^+\rangle_{ab}|\Phi^+\rangle_{cd}|\Psi\rangle_{e1}^{(2)} \rightarrow & \\
\frac{1}{8\sqrt{2}} \{ & (|H\rangle_1|H\rangle_2|H\rangle_3|H\rangle_4 + |H\rangle_1|V\rangle_2|V\rangle_3|H\rangle_4 \\
& + |V\rangle_1|H\rangle_2|H\rangle_3|V\rangle_4 + |V\rangle_1|V\rangle_2|V\rangle_3|V\rangle_4) \\
& \otimes [\alpha(|H\rangle_a|H\rangle_d + |V\rangle_a|V\rangle_d) \\
& + \beta(|H\rangle_a|V\rangle_d + |V\rangle_a|H\rangle_d)] \\
& + (|H\rangle_1|V\rangle_2|H\rangle_3|H\rangle_4 + |H\rangle_1|H\rangle_2|V\rangle_3|H\rangle_4 \\
& - |V\rangle_1|V\rangle_2|H\rangle_3|V\rangle_4 - |V\rangle_1|H\rangle_2|V\rangle_3|V\rangle_4) \\
& \otimes [\alpha(|H\rangle_a|H\rangle_d + |V\rangle_a|V\rangle_d) \\
& - \beta(|H\rangle_a|V\rangle_d + |V\rangle_a|H\rangle_d)] \\
& + (|V\rangle_1|H\rangle_2|H\rangle_3|H\rangle_4 + |V\rangle_1|V\rangle_2|V\rangle_3|H\rangle_4 \\
& + |H\rangle_1|H\rangle_2|H\rangle_3|V\rangle_4 + |H\rangle_1|V\rangle_2|V\rangle_3|V\rangle_4) \\
& \otimes [\alpha(|H\rangle_a|V\rangle_d + |V\rangle_a|H\rangle_d) \\
& + \beta(|H\rangle_a|H\rangle_d + |V\rangle_a|V\rangle_d)] \\
& + (|H\rangle_1|V\rangle_2|H\rangle_3|V\rangle_4 + |H\rangle_1|H\rangle_2|V\rangle_3|V\rangle_4 \\
& - |V\rangle_1|V\rangle_2|H\rangle_3|H\rangle_4 - |V\rangle_1|H\rangle_2|V\rangle_3|H\rangle_4) \\
& \otimes [\alpha(|H\rangle_a|V\rangle_d + |V\rangle_a|H\rangle_d) \\
& - \beta(|H\rangle_a|H\rangle_d + |V\rangle_a|V\rangle_d)] \} \\
& + \frac{\sqrt{3}}{2}|\varphi_{II}\rangle, \tag{7}
\end{aligned}$$

where $|\varphi_{II}\rangle$ is a normalized state including the amplitudes that would lead to unsuccessful cases in which one or more of the eight detectors detect more than one photon.

From Eq. (7) it is clear that a different combination of the detectors receiving exactly one photon leads to a different output state in modes a and d as follows,

$$|\Psi_1\rangle_{ad} = \alpha|0\rangle^{(2)} + \beta|1\rangle^{(2)}, \tag{8}$$

$$|\Psi_2\rangle_{ad} = \alpha|0\rangle^{(2)} - \beta|1\rangle^{(2)}, \tag{9}$$

$$|\Psi_3\rangle_{ad} = \alpha|1\rangle^{(2)} + \beta|0\rangle^{(2)}, \tag{10}$$

$$|\Psi_4\rangle_{ad} = \alpha|1\rangle^{(2)} - \beta|0\rangle^{(2)}. \tag{11}$$

For example, combination of D_{1H} , D_{2H} , D_{3H} and D_{4H} gives the state $|\Psi_1\rangle_{ad}$ as shown in Eq. (8), while combination of D_{1V} , D_{2V} , D_{3H} and D_{4H} gives the state $|\Psi_4\rangle_{ad}$ as shown in Eq. (11). Although the four output states are different, they are locally equivalent. The state $|\Psi_1\rangle_{ad}$ is the expected outcome, i.e. equivalent to $|\Psi\rangle_{e1}^{(2)}$. The

state $|\Psi_2\rangle_{ad}$ is only a phase-flipped version of $|\Psi_1\rangle_{ad}$, which can be transformed to $|\Psi_1\rangle_{ad}$ by implementing the local operation σ_z on both the photons in modes a and d . For the state $|\Psi_3\rangle_{ad}$, a bit-flip occurs, which can be corrected by a local operation σ_x on either of the photons in modes a and d . Both a bit-flip and a phase-flip occur to the state $|\Psi_4\rangle_{ad}$, so the local operation is $\sigma_{z_a} \otimes \sigma_{z_d} \sigma_{x_d}$ or $\sigma_{z_a} \sigma_{x_a} \otimes \sigma_{z_d}$.

Eq. (7) also shows that each output state succeeds with a probability of $1/16$, however, if we accept all the four states and use the classically controlled single-qubit operations as we have shown, then the probability can be increased to $1/4$. In a scaled-up scheme fusion with the qubit state would only proceed when the resource had been successfully constructed. In addition, because of the characteristics of the type-II fusion gate (See Eq. (5)), recovery from unsuccessful fusion of the parity qubit is also possible. Iteration can then improve the probability of success towards unity. Such scale-up would require efficient multi-photon production and quantum memory beyond current capabilities, and hence here we restrict our attention mostly to the basic probabilistic operations (see Section V for a discussion of recovery techniques in a teleportation scenario).

IV. PARITY ENCODED QUANTUM COMPUTATION

It is known that with polarization encoded qubits we can perform any single-qubit unitary operation deterministically with passive linear optical elements. Gates between different photons, like the CNOT gate, can be performed nondeterministically. However, performing gates on the parity encoded states is somewhat different.

It is straightforward to perform any of the gates which can be achieved with the set $\{X_\theta, Z\}$ on the parity encoded states. Here the notation is $X_\theta = \cos(\theta/2)I - i\sin(\theta/2)\sigma_x$ and Z means the σ_z operation. To perform an X_θ rotation on a parity encoded state, we only need to perform the rotation on any of the component qubits because the σ_x rotation on any of the component qubits can change the parity of the encoded state. To perform a Z operation, we need to perform the σ_z operation on all the component qubits as the odd parity states will suffer an overall phase-flip. However, to achieve a universal set of gates we need to add the set $\{Z_{90}, CNOT\}$. Here the notation is $Z_{90} = e^{-i\pi\sigma_z/4}$. We can only perform these gates on parity encoded states nondeterministically.

According to the proposal by Gilchrist *et al.* [4], we give a detailed analysis of how to implement the Z_{90} gate with the re-encoder. The main procedure is that we first perform the Z_{90} gate on one of the component qubits and then re-encode from that qubit. By inserting a quarter-wave plate (QWP) set to 0° in beam e prior to PBS2, we can perform the Z_{90} gate on the photon in mode e .

Then the state in modes e and 1 will be transformed to

$$|\Psi'\rangle_{e1} = \frac{1}{\sqrt{2}}[\alpha(|H\rangle_e|H\rangle_1 + i|V\rangle_e|V\rangle_1) + \beta(|H\rangle_e|V\rangle_1 + i|V\rangle_e|H\rangle_1)]. \quad (12)$$

Based on similar calculations as those used in the description of the re-encoder, we can also get four different output states in modes a and d corresponding to different combinations of the detectors receiving exactly one photon, but the corrections are different for some of the combinations.

For the combination $D_{1H}, D_{2H}, D_{3H}, D_{4H}$, or $D_{1H}, D_{2V}, D_{3V}, D_{4H}$, or $D_{1V}, D_{2V}, D_{3H}, D_{4V}$, or $D_{1V}, D_{2H}, D_{3V}, D_{4V}$, the output state collapses to

$$|\Psi'_1\rangle_{ad} = \alpha|0\rangle^{(2)} + i\beta|1\rangle^{(2)}, \quad (13)$$

which is the expected state. If the combination is $D_{1V}, D_{2H}, D_{3H}, D_{4V}$, or $D_{1V}, D_{2V}, D_{3V}, D_{4V}$, or $D_{1H}, D_{2V}, D_{3H}, D_{4H}$, or $D_{1H}, D_{2H}, D_{3V}, D_{4H}$, the output state will become to

$$|\Psi'_2\rangle_{ad} = \alpha|0\rangle^{(2)} - i\beta|1\rangle^{(2)}, \quad (14)$$

which is a phase-flipped version, so we need a local operation σ_z on both of the two output modes. The combination $D_{1H}, D_{2H}, D_{3H}, D_{4V}$, or $D_{1H}, D_{2V}, D_{3V}, D_{4V}$, or $D_{1V}, D_{2V}, D_{3H}, D_{4H}$, or $D_{1V}, D_{2H}, D_{3V}, D_{4H}$ leads to the output state

$$|\Psi'_3\rangle_{ad} = \alpha|1\rangle^{(2)} + i\beta|0\rangle^{(2)}, \quad (15)$$

which only needs a correction of a local operation σ_x on either of the two output modes. Another combination is $D_{1V}, D_{2H}, D_{3H}, D_{4H}$, or $D_{1V}, D_{2V}, D_{3V}, D_{4H}$, or $D_{1H}, D_{2V}, D_{3H}, D_{4V}$, or $D_{1H}, D_{2H}, D_{3V}, D_{4V}$, which results in the output state

$$|\Psi'_4\rangle_{ad} = \alpha|1\rangle^{(2)} - i\beta|0\rangle^{(2)}, \quad (16)$$

therefore we need a correction $\sigma_{z_a} \otimes \sigma_{z_d} \sigma_{x_d}$ or $\sigma_{z_a} \sigma_{x_a} \otimes \sigma_{z_d}$. The probability of each success output state is again $1/16$, which can also be improved to $1/4$ if we accept all the four output states.

For the operation of the CNOT gate, Gilchrist et al. [4] proposed a procedure similar to the Z_{90} gate. We will not show the detail of the CNOT implementation:

$$|\Psi\rangle_c^{(n)} |\Psi\rangle_t^{(n)} \rightarrow \text{CNOT} |\Psi\rangle_c^{(n)} |\Psi\rangle_t^{(n)}, \quad (17)$$

where $|\Psi\rangle_c^{(n)} (|\Psi\rangle_t^{(n)})$ is the n -qubit parity encoded control (target) state. Again using a type-I fusion gate and a type-II fusion gate we can first implement the operation:

$$|\Psi\rangle_c^{(n)} |\Psi\rangle_t^{(n)} |0\rangle^{(n+1)} \rightarrow \text{CNOT} |\Psi\rangle_c^{(n)} |\Psi\rangle_t^{(n-1)}, \quad (18)$$

and then a re-encoder can encode the target state to a n -qubit parity encoded state. However note that for the first level parity state ($n = 2$), far more than six photons are needed and hence it is beyond the scope of this paper.

V. PARITY ENCODED QUANTUM TELEPORTATION

Another way to understand the re-encoder is in terms of teleportation. Quantum teleportation [14], a way to transfer a quantum state from one place to another, has received much attention since it was presented. It plays an important role in quantum communication [15] and computation [1, 16]. An efficient way to improve the probability of success of teleportation is using parity encoding to encode against the failure which results in a computational basis measurement [1, 2]. Quantum teleportation of an arbitrary two-qubit composite system has been realized in the experiment [17]. This experiment demonstrated teleportation of a two-qubit parity encoded state, but it couldn't show all the features against failure because the Bell measurement was implemented on each of the two qubits individually. Here we give another way to teleport a parity encoded state using the re-encoder, which demonstrates the basic ability to encode against the failure in teleportation.

As illustrated in Fig.2, Alice wants to teleport an unknown parity encoded state $|\Psi\rangle_{e1}^{(2)}$ in modes e and 1 to Bob. To do so, first Alice and Bob share two Bell states $|\Phi^+\rangle_{ab}$ and $|\Phi^+\rangle_{cd}$, where the photons in modes b and c are sent to Alice while the photons in modes a and d are sent to Bob. Alice then carries out the fusion operations used in the re-encoder and tells Bob the measurement results in modes 1, 2, 3 and 4 via classical communication. On receiving these results, with the corrections shown in the description of the re-encoder, Bob can then get the state in modes a and d , which is the same with the teleported state by Alice. As in the re-encoder, the total probability of success of teleportation is also $1/4$.

To explore the procedure of encoding against the failure, we analyze the failure cases in the two fusion gates. If a failure occurs to the measurement in mode 4, Alice can try again the fusion at PBS1 instead of carrying out the fusion at PBS2, so that the state in modes e and 1 will not be destroyed and can still be used unless the measurement in mode 4 succeeds. If a failure occurs to the fusion at PBS2, it will destroy the state in modes e and 1, but that is not a problem for Alice, because she need not make a measurement in mode 1. Instead, she need only re-encode from the state in mode 1, with only a bit-flip correction required depending on the failure results. Note that the proposal in this paper can't be used to recover the initial state from mode 1, because we do not use an encoder to generate the parity encoded state, but that does not affect the role of the re-encoder.

The procedure of recycling of entangled states against the failure can also be implemented for the parity encoded quantum computation, as was done for the cluster computation proposal [18].

VI. GENERATION OF THE THREE ENTANGLED STATES USING PARAMETRIC DOWN-CONVERSION PROCESSES

So far we have considered the situation in which our source deterministically produces three entangled-photon Bell pairs. However in real experiment it may not be the case. Currently, nearly all the entangled-photon sources in LOQC experiments use parametric down-conversion(PDC) [19, 20]. In order to demonstrate the re-encoder we need three entangled-photon pairs, so a six-photon source is required, which is now available in the experiment [17, 21]. We may use three PDC sources, each of which generates an entangled-photon pair.

As we know, PDC is a multi-photon generation process. The probabilities that a n -pair is generated from a single PDC source is the same as that a single pair is generated from n PDC sources [8]. If we first consider three-pair order, we see that when a double-pair is produced in one of the Bell state sources while no pairs are produced in another we can also get the correct fourfold detections but the output states are wrong results with two photons in one of the output modes while no photons in another. However, by specifically using the optical arrangement of Fig.2, and using post-selection, i.e., sixfold coincidence detections of the correct fourfold detections together with the detections of the two output modes to make sure a photon exits in each output mode, can solve this problem. This type of method is currently used in virtually all experiments using PDC.

Another concern is due to higher-order processes in which more than six photons are generated and this can also lead to wrong results even though we use post-selection. In real experiment, the efficiency of generating two photons per pulse from PDC is typically $|\chi|^2 \sim 10^{-4}$. Then the efficiency of six- and eight-photon generation from PDC is $|\chi|^6 \sim 10^{-12}$ and $|\chi|^8 \sim 10^{-16}$. Therefore the eight-photon generation rate is $\sim 10^{-4}$ lower than that of six-photon generation and is negligible. It should be noted that theoretically we assume the detectors are number-resolving, however, in the case of post-selection, conventional detectors are acceptable, since higher-order processes are negligible. Another error source in a real experiment is dark counts of conventional detectors, but that of current detectors is sufficiently small and hence they are negligible in multi-photon coincidence experiments.

From all the discussions above, we believe that with existing technology the proposed re-encoder is able to be performed using PDC sources, linear optical elements, and conventional photon detectors.

VII. MODE-MISMATCH ERRORS

In nonclassical interference experiments a major contribution of nonunit visibility is mode-mismatch. To model mode-mismatch explicit multi-mode calculations

may be used [22], but it becomes very complicated to deal with multi-photon set-ups. In this paper we model mode-mismatch using a simpler approach similar to the analysis by Ralph *et al.* [23]. A rigorous justification of this approach can be found in [24].

As shown in Fig.2, there is nonclassical interference at PBS1 and PBS2. We introduce two parameters η_1 and η_2 ($0 \leq \eta_1, \eta_2 \leq 1$) to quantify the degrees of mode matching between the two input modes of PBS1 and PBS2. We assume that due to mode-mismatch the three initial entangled states become

$$\begin{aligned}
|\Phi^+\rangle_{ab} |\Phi^+\rangle_{cd} |\Psi\rangle_{e1}^{(2)} &\rightarrow \\
&\left(\sqrt{\eta_1} |\Phi^+\rangle_{ab} + \sqrt{1-\eta_1} |\Phi^+\rangle'_{ab} \right) |\Phi^+\rangle_{cd} \\
&\otimes \left(\sqrt{\eta_2} |\Psi\rangle_{e1}^{(2)} + \sqrt{1-\eta_2} |\Psi\rangle''_{e1}^{(2)} \right) \\
= &\sqrt{\eta_1 \eta_2} |\Phi^+\rangle_{ab} |\Phi^+\rangle_{cd} |\Psi\rangle_{e1}^{(2)} \\
&+ \sqrt{(1-\eta_1)(1-\eta_2)} |\Phi^+\rangle'_{ab} |\Phi^+\rangle_{cd} |\Psi\rangle''_{e1}^{(2)} \\
&+ \sqrt{\eta_1(1-\eta_2)} |\Phi^+\rangle_{ab} |\Phi^+\rangle_{cd} |\Psi\rangle''_{e1}^{(2)} \\
&+ \sqrt{(1-\eta_1)\eta_2} |\Phi^+\rangle'_{ab} |\Phi^+\rangle_{cd} |\Psi\rangle_{e1}^{(2)}. \quad (19)
\end{aligned}$$

Here

$$\begin{aligned}
|\Phi^+\rangle'_{ab} &= \frac{1}{\sqrt{2}} (|H\rangle_a |H\rangle'_b + |V\rangle_a |V\rangle'_b), \quad (20) \\
|\Psi\rangle''_{e1}^{(2)} &= \frac{1}{\sqrt{2}} [\alpha (|H\rangle'_e |H\rangle_1 + |V\rangle'_e |V\rangle_1) \\
&\quad + \beta (|H\rangle'_e |V\rangle_1 + |V\rangle'_e |H\rangle_1)], \quad (21)
\end{aligned}$$

where we use the notation $|H\rangle'_b$ ($|V\rangle'_b$) to denote the mode-mismatch state of the photon in mode b , which is distinguishable from the state $|H\rangle_c$ ($|V\rangle_c$) of the photon in mode c . Similarly the mode-mismatch state $|H\rangle''_e$ ($|V\rangle''_e$) is distinguishable from $|H\rangle_d$ ($|V\rangle_d$). Note that although we only introduce the mode-mismatch in a single degree of freedom, this is sufficient to model arbitrary mode-mismatch effects [25].

We can see that there are four distinguishable cases corresponding to the four terms of Eq. (19) and the state transformation for each of them can be given in the same way used in the description of the re-encoder. For simplicity we only give the states which can lead to exactly one photon in the detectors D_{1H} , D_{2H} , D_{3H} and D_{4H} , so the four terms of Eq. (19) evolve such that, the first term:

$$\begin{aligned}
\sqrt{\eta_1 \eta_2} |\Phi^+\rangle_{ab} |\Phi^+\rangle_{cd} |\Psi\rangle_{e1}^{(2)} &\rightarrow \\
&\frac{1}{8} \sqrt{\eta_1 \eta_2} |H\rangle_1 |H\rangle_2 |H\rangle_3 |H\rangle_4 |\Psi\rangle_{ad}^{(2)}, \quad (22)
\end{aligned}$$

the second term:

$$\begin{aligned} & \sqrt{(1-\eta_1)(1-\eta_2)}|\Phi^+\rangle'_{ab}|\Phi^+\rangle_{cd}|\Psi\rangle''_{e1}{}^{(2)} \rightarrow \\ & \frac{1}{8\sqrt{2}}\sqrt{(1-\eta_1)(1-\eta_2)}\left[\alpha|H\rangle_1|H\rangle_2'|H\rangle_3|H\rangle_4|+\rangle_a|+\rangle_d \right. \\ & \quad +\beta|H\rangle_1|H\rangle_2''|H\rangle_3'|H\rangle_4|+\rangle_a|+\rangle_d \\ & \quad +\alpha|H\rangle_1|H\rangle_2|H\rangle_3''|H\rangle_4'|-\rangle_a|-\rangle_d \\ & \quad \left. -\beta|H\rangle_1|H\rangle_2''|H\rangle_3|H\rangle_4'|-\rangle_a|-\rangle_d\right], \end{aligned} \quad (23)$$

the third term:

$$\begin{aligned} & \sqrt{\eta_1(1-\eta_2)}|\Phi^+\rangle_{ab}|\Phi^+\rangle_{cd}|\Psi\rangle''_{e1}{}^{(2)} \rightarrow \\ & \frac{1}{8}\sqrt{\eta_1(1-\eta_2)}\left[\alpha|H\rangle_1|H\rangle_2|H\rangle_3''|H\rangle_4|0\rangle_{ad}^{(2)} \right. \\ & \quad \left. +\beta|H\rangle_1|H\rangle_2''|H\rangle_3|H\rangle_4|1\rangle_{ad}^{(2)}\right], \end{aligned} \quad (24)$$

the fourth term:

$$\begin{aligned} & \sqrt{(1-\eta_1)\eta_2}|\Phi^+\rangle'_{ab}|\Phi^+\rangle_{cd}|\Psi\rangle_{e1}{}^{(2)} \rightarrow \\ & \frac{1}{8\sqrt{2}}\sqrt{(1-\eta_1)\eta_2}\left[\alpha|H\rangle_1|H\rangle_2'|H\rangle_3|H\rangle_4|+\rangle_a|+\rangle_d \right. \\ & \quad +\beta|H\rangle_1|H\rangle_2|H\rangle_3'|H\rangle_4|+\rangle_a|+\rangle_d \\ & \quad \left. +(\alpha-\beta)|H\rangle_1|H\rangle_2|H\rangle_3|H\rangle_4'|-\rangle_a|-\rangle_d\right], \end{aligned} \quad (25)$$

from which we can see that the first term leads the output state in modes a and d to the expected state $|\Psi\rangle_{ad}^{(2)}$, while the other terms lead to a mixed state in modes a and d . For other combinations of detectors as shown in the analysis of the re-encoder we can also get similar results with corresponding corrections.

Based on these observations, the density matrix of the output state can be given by

$$\begin{aligned} \hat{\rho}_{out}^{(\pm)} &= \frac{1}{64}\eta_1\eta_2|\Psi\rangle_{ad}^{(2)}\langle\Psi|_{ad}^{(2)} \\ & +\frac{1}{128}(1-\eta_1)|\pm\rangle_a\langle\pm|_a\otimes|\pm\rangle_d\langle\pm|_d \\ & +\frac{1}{128}(1-\eta_1)[1\mp 2\text{Re}(\alpha\beta^*)\eta_2] \\ & \quad \times|\mp\rangle_a\langle\mp|_a\otimes|\mp\rangle_d\langle\mp|_d \\ & +\frac{1}{64}\eta_1(1-\eta_2)|\alpha|^2|0\rangle_{ad}^{(2)}\langle 0|_{ad}^{(2)} \\ & +\frac{1}{64}\eta_1(1-\eta_2)|\beta|^2|1\rangle_{ad}^{(2)}\langle 1|_{ad}^{(2)}, \end{aligned} \quad (26)$$

where $\hat{\rho}_{out}^{(+)}$ corresponds to the output state with no correction or with the bit-flip correction, while $\hat{\rho}_{out}^{(-)}$ corresponds to the output state after the phase-flip correction or after both the phase-flip and the bit-flip correction.

The probability of success is given by

$$P^{(\pm)} = \text{tr}\left(\hat{\rho}_{out}^{(\pm)}\right) = \frac{1}{64}[1\mp(1-\eta_1)\eta_2\text{Re}(\alpha\beta^*)]. \quad (27)$$

The fidelity is given by

$$F^{(\pm)} = \frac{\langle\Psi|^{(2)}\hat{\rho}_{out}^{(\pm)}|\Psi\rangle^{(2)}}{\text{tr}\left(\hat{\rho}_{out}^{(\pm)}\right)}, \quad (28)$$

where,

$$\begin{aligned} \langle\Psi|^{(2)}\hat{\rho}_{out}^{(\pm)}|\Psi\rangle^{(2)} &= \\ & \frac{1}{128}\{1+\eta_1-4\eta_1(1-\eta_2)|\alpha\beta|^2 \\ & \quad \mp(1-\eta_1)\eta_2\text{Re}(\alpha\beta^*)[1\mp 2\text{Re}(\alpha\beta^*)]\}. \end{aligned} \quad (29)$$

From Eqs. (27), (28) and (29) we can see that the fidelity depends on not only the mode matching parameters but also the input states. If we integrate over the whole space of the pure input state, we find that the average fidelity is the same for $F^{(\pm)}$. To show that, we make the substitution,

$$\alpha = \cos\frac{\theta}{2}, \quad (30)$$

$$\beta = e^{i\phi}\sin\frac{\theta}{2}. \quad (31)$$

The average fidelity can then be given by

$$\begin{aligned} F_{ave} &= \frac{1}{4\pi}\int_0^{2\pi}d\phi\int_0^\pi F^{(\pm)}\sin\theta d\theta \\ &= \frac{1}{4\pi}\int_{-\frac{\pi}{2}}^{\frac{\pi}{2}}d\phi\int_0^\pi (F^{(+)}+F^{(-)})\sin\theta d\theta. \end{aligned} \quad (32)$$

In Fig.3 we plotted the average fidelity as a function of mode matching parameters η_1 and η_2 . If we assume $\eta_1 = \eta_2 = \eta$, the relationship between the average fidelity and η is shown in Fig.4.

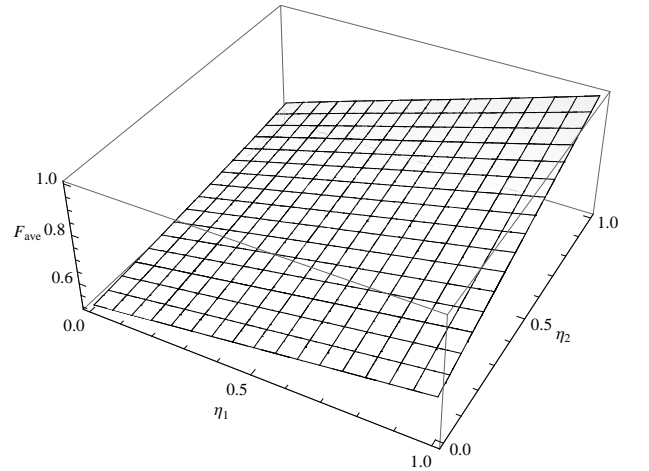


FIG. 3: Average fidelity F_{ave} as a function of mode matching parameters η_1 and η_2 .

Similar analysis of mode-mismatch can also be implemented to the Z_{90} operation. The density matrix of the

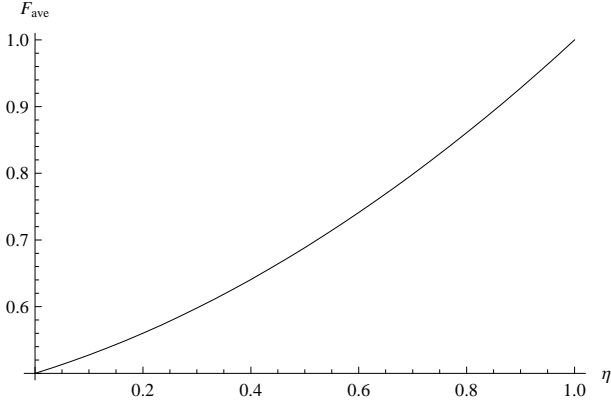


FIG. 4: Average fidelity F_{ave} as a function of η , assuming mode matching parameters $\eta_1 = \eta_2 = \eta$.

output state after the Z_{90} operation is given by

$$\begin{aligned}
\tilde{\rho}_{out}^{(\pm)} &= \frac{1}{64} \eta_1 \eta_2 |\Psi'_1\rangle_{ad} \langle \Psi'_1|_{ad} \\
&\quad + \frac{1}{128} (1 - \eta_1) |\pm\rangle_a \langle \pm|_a \otimes |\pm\rangle_d \langle \pm|_d \\
&\quad + \frac{1}{128} (1 - \eta_1) [1 \mp 2\text{Im}(\alpha\beta^*) \eta_2] \\
&\quad \quad \quad \times |\mp\rangle_a \langle \mp|_a \otimes |\mp\rangle_d \langle \mp|_d \\
&\quad + \frac{1}{64} \eta_1 (1 - \eta_2) |\alpha\rangle_{ad}^{(2)} \langle 0|_{ad}^{(2)} \\
&\quad + \frac{1}{64} \eta_1 (1 - \eta_2) |\beta\rangle_{ad}^{(2)} \langle 1|_{ad}^{(2)}, \tag{33}
\end{aligned}$$

where $|\Psi'_1\rangle_{ad}$ is the expected state as shown in Eq. (13) and $\tilde{\rho}_{out}^{(+)}$ corresponds to the output states with no correction or with the bit-flip correction, while $\tilde{\rho}_{out}^{(-)}$ corresponds to the output state after the phase-flip correction or after both the phase-flip and the bit-flip correction.

The probability of success is given by

$$\tilde{P}^{(\pm)} = \text{tr} \left(\tilde{\rho}_{out}^{(\pm)} \right) = \frac{1}{64} [1 \mp (1 - \eta_1) \eta_2 \text{Im}(\alpha\beta^*)]. \tag{34}$$

The fidelity is also given by

$$\tilde{F}^{(\pm)} = \frac{\langle \Psi'_1 |_{ad} \tilde{\rho}_{out}^{(\pm)} | \Psi'_1 \rangle_{ad}}{\text{tr} \left(\tilde{\rho}_{out}^{(\pm)} \right)}, \tag{35}$$

where,

$$\begin{aligned}
\langle \Psi'_1 |_{ad} \hat{\rho}_{out}^{(\pm)} | \Psi'_1 \rangle_{ad} &= \\
&\quad \frac{1}{128} \{ 1 + \eta_1 - 4\eta_1(1 - \eta_2) |\alpha\beta|^2 \\
&\quad \quad \mp (1 - \eta_1) \eta_2 \text{Im}(\alpha\beta^*) [1 \mp 2\text{Im}(\alpha\beta^*)] \}. \tag{36}
\end{aligned}$$

The average fidelity can also be given by

$$\begin{aligned}
\tilde{F}_{\text{ave}} &= \frac{1}{4\pi} \int_0^{2\pi} d\phi \int_0^\pi \tilde{F}^{(\pm)} \sin \theta d\theta \\
&= \frac{1}{4\pi} \int_{-\frac{\pi}{2}}^{\frac{\pi}{2}} d\phi \int_0^\pi (F^{(+)} + F^{(-)}) \sin \theta d\theta. \tag{37}
\end{aligned}$$

For a specific input state, the fidelity may be different in the Z_{90} operation compared with the re-encoder, but from Eq. (32) and (37) we can see that the average fidelity is the same.

VIII. CONCLUSIONS

We have considered the problem of demonstrating the basic elements of parity encoded linear optical quantum computation. We have shown that operations on the smallest non-trivial example, the two-photon parity state, can be demonstrated using a six-photon parametric down-conversion source. Our proposal allows demonstration of basic re-encoding, including explicitly the construction of the resource state. The basic re-encoder is key in loss tolerant operation [12] as it acts as an error detector for loss. In effect the re-encoder performs a quantum non-demolition measurement of photon number on the parity qubit. The re-encoder can also be used to implement arbitrary single qubit gates, which we also discussed and the it can also be understood as a process of teleportation. We have shown that multi-photon down-conversion in events can be post-selected out of the data. We have also considered the effect of mode-mismatch on the operation of our gates and shown that it leads to an approximately linear reduction in fidelity as a function of mode overlap.

Experimental demonstrations play a crucial role in evaluating and testing the relative merits of different quantum processing schemes. We hope that our proposal will stimulate such investigations of parity state LOQC.

Acknowledgments

YXG was funded by National Fundamental Research Program (Grant No. 2006CB921907), National Natural Science Foundation of China (Grant No. 60121503 and No. 60621064), Innovation Funds from Chinese Academy of Sciences, International Cooperate Program from CAS and Ministry of Science & Technology of China. AJFH and TCR were supported by the DTO-funded U.S. Army Research Office Contract No. W911NF-05-0397 and the Australian Research Council.

-
- [1] E. Knill, R. Laflamme, and G. J. Milburn, *Nature (London)* **409**, 46 (2001).
- [2] P. Kok, W. J. Munro, K. Nemoto, T. C. Ralph, J. P. Dowling, and G. J. Milburn, *Rev. Mod. Phys.* **79**, 135 (2007).
- [3] M. A. Nielsen, *Phys. Rev. Lett.* **93**, 040503 (2004).
- [4] A. Gilchrist, A. J. F. Hayes, and T. C. Ralph, *Phys. Rev. A* **75**, 052328 (2007).
- [5] J. L. O'Brien, G. J. Pryde, A. G. White, T. C. Ralph, and D. Branning, *Nature (London)* **426**, 264 (2003).
- [6] S. Gasparoni, J.-W. Pan, P. Walther, T. Rudolph, and A. Zeilinger, *Phys. Rev. Lett.* **93**, 020504 (2004).
- [7] T. B. Pittman, M. J. Fitch, B. C. Jacobs, and J. D. Franson, *Phys. Rev. A* **68**, 032316 (2003).
- [8] P. Walther, K. J. Resch, T. Rudolph, E. Schenck, H. Weinfurter, V. Vedral, M. Aspelmeyer, and A. Zeilinger, *Nature (London)* **434**, 169 (2005).
- [9] R. Prevedel, P. Walther, F. Tiefenbacher, P. Böhi, R. Kaltenbaek, T. Jennewein, and A. Zeilinger, *Nature (London)* **445**, 65 (2007).
- [10] J. L. O'Brien, G. J. Pryde, A. G. White, and T. C. Ralph, *Phys. Rev. A* **71**, 060303 (2005).
- [11] T. B. Pittman, B. C. Jacobs, and J. D. Franson, *Phys. Rev. A* **71**, 052332 (2005).
- [12] T. C. Ralph, A. J. F. Hayes, and A. Gilchrist, *Phys. Rev. Lett.* **95**, 100501 (2005).
- [13] A. J. F. Hayes, A. Gilchrist, and T. C. Ralph, *J. Opt. B: Quantum Semiclass. Opt.* **6**, 533 (2004).
- [14] C. H. Bennett, G. Brassard, C. Crépeau, R. Jozsa, A. Peres, and W. K. Wootters, *Phys. Rev. Lett.* **70**, 1895 (1993).
- [15] H. J. Briegel, W. Dür, J. I. Cirac, and P. Zoller, *Phys. Rev. Lett.* **81**, 5932 (1998).
- [16] D. Gottesman and I. L. Chuang, *Nature (London)* **402**, 390 (1999).
- [17] Q. Zhang, A. Goebel, C. Wagenknecht, Y. A. Chen, B. Zhao, T. Yang, A. Mair, J. Schmiedmayer, and J. W. Pan, *Nat. Phys.* **2**, 678 (2006).
- [18] D. E. Browne and T. Rudolph, *Phys. Rev. Lett.* **95**, 010501 (2005).
- [19] P. G. Kwiat, K. Mattle, H. Weinfurter, A. Zeilinger, A. V. Sergienko, and Y. Shih, *Phys. Rev. Lett.* **75**, 4337 (1995).
- [20] P. G. Kwiat, E. Waks, A. G. White, I. Appelbaum, and P. H. Eberhard, *Phys. Rev. A* **60**, R773 (1999).
- [21] C. Y. Lu, X. Q. Zhou, O. Gühne, W. B. Gao, J. Zhang, Z. S. Yuan, A. Goebel, T. Yang, and J. W. Pan, *Nat. Phys.* **3**, 91 (2007).
- [22] P. P. Rohde and T. C. Ralph, *Phys. Rev. A* **71**, 032320 (2005).
- [23] T. C. Ralph, N. K. Langford, T. B. Bell, and A. G. White, *Phys. Rev. A* **65**, 062324 (2002).
- [24] P. P. Rohde, W. Mauerer, and C. Silberhorn, *New J. Phys.* **9**, 91 (2007).
- [25] P. P. Rohde, G. J. Pryde, J. L. O'Brien, and T. C. Ralph, *Phys. Rev. A* **72**, 032306 (2005).